How an Actin Network Might Cause Fountain Streaming and Nuclear Migration in the Syncytial *Drosophila* Embryo

George von Dassow and Gerold Schubiger

Department of Zoology, University of Washington, Seattle, Washington 98195

Abstract. We show here using time-lapse video tapes that cytoplasmic streaming causes nuclear migration along the anterior-posterior axis (axial expansion) in the early syncytial embryo of *Drosophila melanogaster.* Using confocal microscopy and labeled phalloidin we explore the distribution of F-actin during axial expansion. We find that a network of F-actin fibers fills the cytoplasm in the embryo. This actin network partially disassembles around the nuclei during axial expansion. Our observations of normal development, fixed embryos, and drug injection experiments indicate that disassembly of the actin network generates cytoplasmic movements. We suggest that the cell cycle regulates disassembly of the actin network, and that this process may be mediated directly or indirectly by the microtubules. The cytoplasmic movements we observe during axial expansion are very similar to fountain streaming in the pseudopod of amoebae, and by analogy with the pseudopod we propose a working hypothesis for axial expansion based on solation-contraction coupling within the actin network.

PROGRESS in understanding the role of the actin cytoskeleton in cell crawling and cell shape change includes the identification of many proteins that regulate the state of actin (for review see Stossel, 1993) and the development of several models of actin-dependent cell shape changes including cytokinesis (White and Borisy, 1983) and amoeboid motion (Allen, 1973; Odell, 1977; Taylor and Fechheimer, 1982). All these models make use of the contractile and dynamic nature of actin/myosin networks. Despite these advances, it remains largely unknown what stimuli initiate reorganization of the actin cytoskeleton or how reorganization is transmitted to organelles and the plasma membrane.

Many of the concepts regarding the function of actin/myosin networks in nonmuscle cells originate with studies of amoeboid motion. Allen (1961) defined amoeboid motion as any cellular movement caused by active cytoplasmic streaming, and outlined the importance of cytoplasmic streaming to cell motility and to morphogenesis of nonmotile cells such as blastomeres of animal embryos. Experimental study of cytoplasmic streaming during pseudopod extension in giant amoebae such as *Chaos carolinensis* indicates that the presence of contractile elements and the transition between "gel" and "sol" states of the cytoplasm are essential for explaining amoeboid motion (Allen, 1961). It has been possible to directly integrate observations on the living pseudopod with the biochemical and physical properties of actin, myosin, and other actin-binding proteins (Odell, 1977; Taylor and Fechheimer, 1982), and to apply the conclusions to a variety of cell types and behaviors (Oster and Odell, 1984; Janson et al., 1991; Kolega et al., 1991; Janson and Taylor, 1993; Giuliano and Taylor, 1994).

Drosophila melanogaster embryos present an ideal system in which to study the cytoskeleton; they are large, readily available single cells with a simple shape, and they are both experimentally and genetically accessible. In the syncytial preblastoderm period we distinguish three phases of nuclear migration (see Fig. 1). Nuclear division initiates in the anterior center of the egg. During the first three mitotic cycles, nuclei remain in a roughly spherical arrangement that moves slowly posterior. In cycles 4–6, nuclei spread out along the long axis of the embryo in a migration termed axial expansion, forming an ellipsoid in which the nuclei space themselves evenly and equidistant from the cortex (Baker et al., 1993). During the remaining preblastoderm divisions, the ellipsoid expands until nuclei reach the surface at cycle 10 (cortical migration; Foe and Alberts, 1983; Baker et al., 1993). Zalokar and Erk (1976) showed that axial expansion depends on microfilament function. In contrast, they showed that cortical migration is microtubule dependent. Baker et al. (1993) revealed that cortical migration and axial expansion also differ in velocity of nuclear migration and in cell cycle phase in which migration takes place, and proposed that an extensive network of microtubules pushes nuclei to the surface.

In this study we analyze axial expansion, and deduce from the observations we present a working hypothesis for axial expansion related to Allen's "frontal contraction" theory for

Address all correspondence to Dr. Gerold Schubiger, Department of Zoology, University of Washington, Seattle, WA 98195. Telephone: (206) 543-8159; FAX: (206) 543-3041.

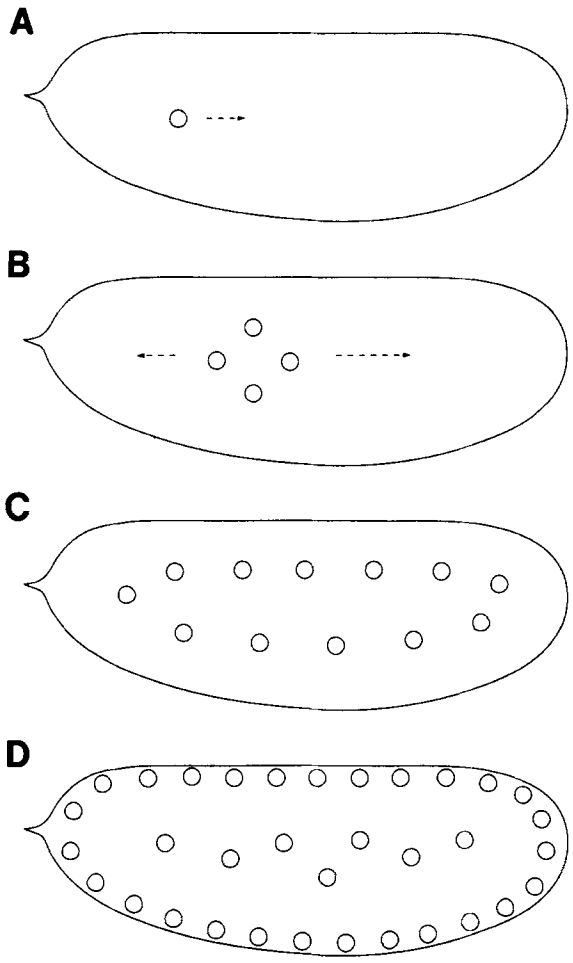

Figure 1. Summary of preblastoderm nuclear migrations. (*A*) Cycle 1. Pronuclei meet in the anterior center of the egg. Arrow indicates direction of migration during cycle 1–3. (*B*) Cycle 4. Nuclei are confined to a spherical region anterior of center. Arrows indicate direction of migration during axial expansion. (*C*) Cycle 7. Nuclei arranged in an ellipsoid equidistant from the cortex. (*D*) Cycle 10. Nuclei arranged in a monolayer under the plasma membrane. Some nuclei remain in the center and become yolk nuclei.

pseudopod extension (Allen, 1973; Odell, 1977). We report first observations of living embryos, demonstrating that cytoplasmic streaming similar to that observed in the pseudopod accompanies axial expansion. Previous reports demonstrate that microfilament inhibitors block axial expansion (Zalokar and Erk, 1976; Hatanaka and Okada, 1991). Hatanaka and Okada (1991) also explored the distribution of F-actin during axial expansion, and reported differences in F-actin distribution between wild-type embryos and embryos from three maternal effect mutant lines in which axial expansion is inhibited. We reexamine the distribution of F-actin using an improved method which reveals dynamic features of the actin cytoskeleton not observed previously. We find that microfilaments form an extensive dynamic network throughout the cytoplasm that changes in concert with the cell cycle. The network "melts" around the nuclei during interphase and prophase, which is also the time when cytoplasmic streaming and axial expansion occur. Finally, we discuss the existing evidence for solation-induced contraction of actin/myosin gels and interpret our observations in light of the solation-contraction coupling hypothesis (Taylor and Fechheimer, 1982). We conclude that local melting of the actin cytoskeleton stimulates the cytoplasmic streaming that stretches and squeezes the array of nuclei such that they spread out along the long axis of the embryo.

Materials and Methods

Embryos

To eliminate overaged embryos, eggs from adult females (Sevelen strain) were precollected and discarded according to the following schedule: 1 h on new food, 30 min on agar plates, 2 × 15 min on agar plates. For all collections, we used 2% agar plates flavored with yeast and acetic acid. Eggs were then collected and aged at 25°C. Embryos were dechorionated in 50% bleach and fixed in a bilayer of fixative under heptane. Fixative was replaced with several rinses of PBS, and embryos were stored not more than 2 d at 4°C under heptane. Embryos must be hand-devitellinized to stain with fluorophore-conjugated phallotoxins; methanol treatment at any stage abolishes binding of phallotoxins to F-actin. Devitellinized embryos were then stored in PBSTx (PBS + 0.1% Triton X-100) at 4°C. Injected embryos were similarly treated.

We tried several fixatives, including full-strength formalin and 8% paraformaldehyde. Buffering either fixative made fixation more reliable, and addition of detergent (0.1% NP-40) helped prevent the vitelline membrane from becoming fixed to the embryo surface. All fixatives preserved microfilaments satisfactorily and were amenable to phalloidin staining. Most embryos shown in this paper were fixed for 10–15 min either in full-strength formalin or in a solution of nine parts formalin, one part stock solution of 1 M Hepes pH 6.9 + 0.5 M EGTA, made to 0.1% NP-40.

Live Video Analysis

Timed embryos were dechorionated by hand and mounted on a slide under halocarbon oil or under Volatef low viscosity oil (3S) with a coverslip. Embryos were videotaped under DIC optics using a Nikon Microphot, 20× dry or 40× water-immersion lens, Hamamatsu Newvicon C2400 video camera with electronic gain and offset controls, and a Gyyr time-lapse video recorder. Gain and offset were adjusted for optimal visualization of energids or particles. Embryos were recorded at 36× real time. Measurements and traces were made directly from the monitor onto acetate sheets. To make energid tracings (an energid is a nucleus and its surrounding cytoplasm), the positions (approximate centers) of 4–7 energids were marked before movement on an acetate sheet attached to the monitor. They were marked again as they stopped moving. Energids were included only if they remained in the plane of focus throughout the expansion period. The traces were converted to vectors using NIH Image, a freeware image analysis program. We estimated the distance traveled inward by lateral energids by multiplying the inward component of the measured vector (expressed as a fraction of egg length) and the approximate length of an embryo (450 μm). While energids and gross patterns of cytoplasmic flow are best visualized under DIC optics with a 20× lens and the condenser turned slightly, particle tracing requires a 40× lens. To trace particle movements during fountain streaming, embryos were videotaped with DIC adjusted for optimal resolution of particles near the cortex. Under these conditions energids are difficult to distinguish. Individual particles were traced one at a time over a 5-min period in which fountain streaming occurred; a mark was made on acetate every minute for each particle, and the tape was then replayed until about 30 particles had been traced in each embryo.

Embryo Injections

Injections were performed as described previously (Baker et al., 1993; Schubiger and Edgar, 1994). Cytochalasin D (CytD)[1] was injected at 250 μg/ml in 1% DMSO, phalloidin (phl) at 6 mg/ml and at 6 μg/ml in water, and cycloheximide (CYH) at a concentration of 1 mg/ml in injection buffer (Weir et al., 1988; injection buffer is 5 mM KCl, 0.1 M $NaPO_4$, pH 6.5); intracellular concentration after injection is estimated to be a 50- or 100-

1. *Abbreviations used in this paper*: CytD, cytochalasin D; CYH, cycloheximide; MTOC, microtubule-organizing center; phl, phalloidin.

fold dilution of the injected concentration (Foe and Alberts, 1983). After injection, embryos were incubated in a humid chamber. Before fixation, the oil was removed and the embryos rinsed off the coverslip using several spritzes of heptane.

Antibody and Phalloidin Staining

Nuclei were visualized using a RITC-conjugated monoclonal anti-histone antibody (Baker et al., 1993). Embryos were blocked in 5% normal goat serum in PBSTx for 30 min at room temperature, and then incubated with antibody solution for 3–6 h at room temperature or overnight at 4°C. Microtubules were visualized with a monoclonal antibody to alpha-tubulin (Amersham Corp., Arlington Heights, IL) and a BODIPY-FL conjugated goat anti-mouse secondary (Molecular Probes Inc., Eugene, OR). Embryos were washed extensively with PBSTx before counterstaining with fluorophore-conjugated phallotoxins.

We used FITC-conjugated phalloidin (FITC-phl), or either BODIPY-558/568 (BR) or BODIPY-FL (BFL) phallicidin to stain F-actin (Molecular Probes). Initial preparations used FITC-phl; however, we found that BODIPY conjugates yielded superior signal. Hand-devitellinized embryos stored in PBSTx were first stained with anti-histone or anti-tubulin antibody, and then treated at room temperature for 30 min–2 h with 0.1–0.2 ml of fluorophore-conjugated phallotoxin at 5–10 U/ml in PBSTx. Variation within these parameters did not affect staining. However, inclusion of detergent (0.1% Triton X-100) in the staining reaction was essential for penetration of phl into the interior of the embryo. Embryos were washed after staining, and mounted in Murray Mounting Medium, a 2:1 mixture of benzyl benzoate and benzyl alcohol. To mount phl-stained embryos in this medium, it was necessary to dehydrate embryos through an isopropanol series, rather than with methanol.

Confocal Microscopy

Samples were examined using a MRC-600 confocal microscope (BioRad Labs., Hercules, CA). Most images presented here were collected using a Plan Apochromatic 60x oil-immersion lens (Nikon). The aperture was set such that successive sections 1 μm apart were 1-μm thick and barely overlapping. Images were collected using double-channel filters, but with a single laser line active at a time to eliminate bleedthrough. Black level and gain were set such that (*a*) a histogram of the image had a single, smooth peak, (*b*) background outside the embryo registered just above zero (~2% of the signal range), and (*c*) fewer than 1% of the pixels were saturated. In none of the images we present were any convolution filters applied after collection; the only filtering applied was the Kalman averaging during the collection of sections. Where indicated, images represent compilations of successive optical sections.

When describing the morphology of F-actin in the embryo, we used the word "filament" to refer to a single actin filament only. Confocal microscopy does not resolve individual actin filaments, and we use the work "fiber" to refer to any linear element (probably comprising many actin filaments) visible in optical sections of phl-stained embryos. Cell cycle phases are defined by the morphology of histone-stained nuclei or by the microtubule configuration (Baker et al., 1993). Histone staining allows one to determine early interphase (small smooth nuclei), late interphase (larger smooth nuclei), prophase (round nuclei with condensing chromatids), metaphase (condensed chromatids in equatorial plane), anaphase (separating chromatids), and telophase (paired, smooth, and tear-shaped nuclei).

F-Actin Intensity Measurements

We collected a single medial optical section from each of 20 embryos in cycles 5 or 6 using the confocal microscope. To avoid photobleaching, we collected only from embryos that had not been examined previously. Each section was taken at the medial optical level, and analyzed using NIH Image. We compared the intensity of staining in the nuclear region with the intensity in the peripheral region (see Fig. 8 *A*). Within these two regions of each embryo, we measured the mean intensity within a series of areas 50 pixels (13.75 μm) square. We measured 11–17 non-overlapping areas per embryo from the peripheral region, and 8–13 within the nuclear region. We made this large number of measurements to sample both regions throughout every image. In choosing areas within the peripheral region, we avoided the bright cortical layer by several microns. We similarly avoided the central domain and the actin caps in the nuclear region (see text for definitions). An overall mean was computed for each region within a given embryo. Fig. 8 *B* presents this data as the difference (expressed as a percentage) between the overall mean signal level in the peripheral region and the nuclear region.

We assessed the contribution to our measurements from two different sources of artifact: background staining or autofluorescence within the sample, and differences in signal intensity due to thickness of the sample between the medial level and the lens. For the former, we reasoned that large yolk spheres should exhibit no specific phl staining within their interior. We measured the mean intensity in the center of several of the larger yolk platelets in each embryo; this value ranged from 5–15% of the signal range. We also measured the mean intensity of signal in unstained embryos, and obtained values from 10–20% of the signal range (unstained cytoplasm is more autofluorescent than yolk). Since the mean intensities of phalloidin staining we measured are generally 30–50% of the signal range, autofluorescence and yolk spheres contribute a very significant baseline. However, we have not subtracted this baseline from the data and images we present because leaving it in biases the data against our conclusions. To address the second point, we measured the diminution of signal when focusing from the near to the far side of several embryos in the sample. We estimated the amount of signal loss in the nuclear region based on this measure, and determined that sample shape can contribute no more than 5–10% loss of signal between the two regions of interest.

Fiber Counts

To generate images from which we could trace fibers, we collected several confocal optical sections from the medial plane of each of 13 embryos. These sections were collected using a 60× lens with the confocal microscope's zoom function set to 3×. After collection, images were analyzed using NIH Image. Two square areas 150 pixels (13.75 μm) wide were chosen from each of the two regions (as above) in each embryo. Each area was then labeled and traced onto acetate sheets attached to the monitor.

Results

Cytoplasmic Flow Motivates Axial Expansion

We have analyzed cytoplasmic and cortical movements during axial expansion in time-lapse videotapes of living embryos. A nucleus and its associated cytoplasm appear as a light sphere (energid) against the yolky deep cytoplasm (Fig. 2, *A–C*). Energids become difficult to distinguish as the nuclei enter metaphase (Fig. 2 *C*), and they reappear and double in number in telophase. We can observe movements of cytoplasm because it is densely packed with yolk spheres and other organelles. In all of ten videos of wild-type embryos that we analyzed, stereotypical cytoplasmic movements accompany axial expansion (Fig. 2 *D* and Table I). Rapid flow of the deep cytoplasm from the center of the embryo toward the poles accompanies poleward migration of energids. At the same time, peripheral cytoplasm flows toward the middle region of the embryo. The waves meet slightly anterior to the middle of the embryo (58 ± 5% EL in cycle 4, 56 ± 4% EL in cycle, 5, 55 ± 4% EL in cycle 6; Table I) and cytoplasm flows inward. Because of its appearance, we refer to the bidirectional flow of deep and peripheral cytoplasm as "fountain streaming," using the term from amoeba literature (Allen, 1973). The inflow of peripheral cytoplasm gives the impression of constricting the deep cytoplasm so we refer to the location where inflow occurs as the "constriction point." Reverse cytoplasmic movements accompany a slight retraction of the energids that occurs after each expansion (Fig. 2 *E*).

In all ten recordings we analyzed, energids did not undergo expansion until cycle 4 and did not expand after cycle 6, nor was bidirectional fountain streaming observed until cycle 4 or after cycle 6. Table I presents assessments of cytoplasmic streaming and axial expansion during cycles 4–6 in

the ten recordings. During cycle 4, fountain streaming is less extensive than in cycles 5 and 6. During cycle 4, retraction is often equivalent in degree to expansion and in some cases the energids return to their initial positions, whereas in cycle 5 and 6, cytoplasmic and energid movements are more extensive during expansion than during retraction. In all recordings, deep cytoplasm and energids move together. In two cases, the cytoplasm flowed unidirectionally toward the anterior during cycle 6; all visible energids correspondingly moved anteriorly. Thus, birectional fountain streaming and expansion were perfectly correlated and unique to cycles 4–6. Cytoplasmic movements occurring before cycle 4 or af-

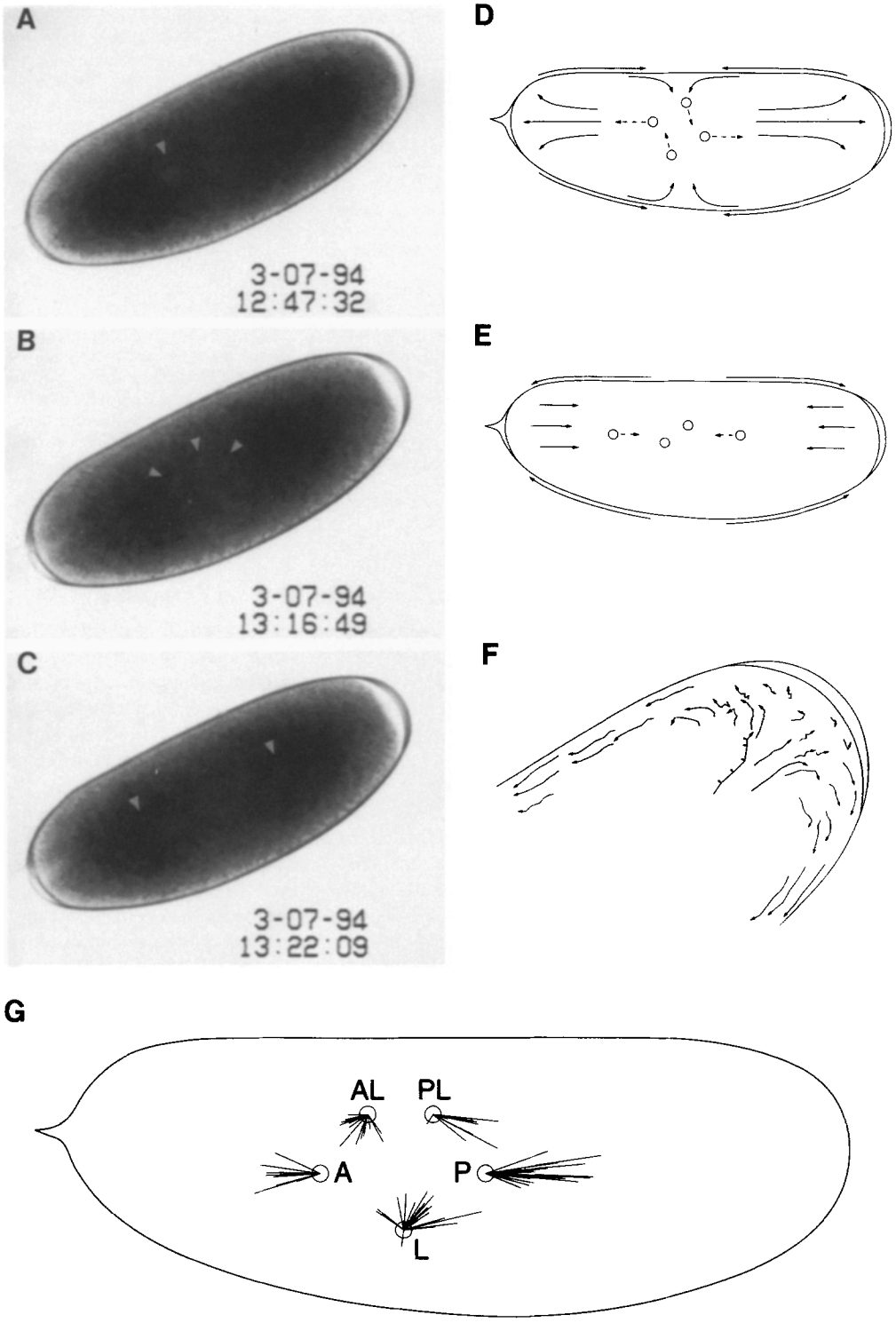

Figure 2. Cytoplasmic and nuclear movements during axial expansion in living embryos. Anterior is to the left. (*A*, *B*, and *C*) Frames from a time-lapse video of a wild-type embryo—early (cycle 2, *A*), preexpansion (early 5, *B*), and postexpansion (late cycle 5, *C*). In each embryo, only some of the energids, usually about half in cycles 4–6, are visible at any time. The energids start in the anterior portion of the egg (*A*; *arrowhead*), and remain within a sphere until axial expansion (*B*; *arrowheads* indicate three of the several visible energids). Energids are more distinct in *B* than in *C*; in *C*, expansion has taken place, and energids have become difficult to discern, indicating entry into metaphase. Arrowheads mark the positions of the anterior- and posterior-most energids as they disappear from view. (*D* and *E*). Diagrams of cytoplasmic movements during cycles 4–6. (*D*) Bi-directional fountain streaming. (*F*) Retraction. Peripheral material spreads away from the middle, and deep cytoplasm compresses from the poles inward, pushing back the energids slightly. (*F*) Tracing made from a higher magnification recording of the posterior pole during extension in cycle 5. The first mark in each particle trail was made immediately before streaming began. A mark was made each minute until streaming ceased. Each trail represents the entire 5-min period in which movement occurred in this embryo. Note both lack of movement by particles near the polar cortex and the circulation of particles moving from the deep cytoplasm into the periphery. (*G*) Energid vectors, cycles 4 and 5. Each line represents a vector (angle relative to the midline, distance in percent egg length) traveled by a single energid from one of 12 analyzed recordings of extension. Vectors are grouped by classification of the energids as *A* (anterior), *P* (posterior), *L* (lateral), or *AL* or *PL* (anterior- or posterior-lateral). All lateral energids except one move toward the midline. Note that the posterior energid vectors are longer than the anterior vectors.

Table I. Cytoplasmic Streaming Correlates with Axial Expansion

	Cy4			Cy5			Cy6		
	Fount	Ret	CP	Fount	Ret	CP	Fount	Ret	CP
			% EL			% EL			% EL
1	nr	nr	nr	++	+	56	++	±	56
2	+	comp	59	++	+	54	++	−	59
3	+	+	64	++	+	64	++	±	59
4	+	+	57	++	+	57	++	−	49
5	++	+	54	++	−	59	++	+	51
6	+	±	64	++	+	58	++	−	58
7	+	comp	61	++	+	55	uni(a)	−	na
8	++	comp	58	++	±	58	++	±	58
9	++	+	49	++	±	49	++	−	49
10	++	+	53	++	+	53	uni(a)	−	na
Mean (SD)			58 (5)			56 (4)			55 (4)

* 1-10 refer to ten individual recordings.
Cy4, *cy5*, *Cy6*, cycles 4, 5, 6; *Fount*, bidirectional fountain streaming; *Ret*, retraction; *CP*, constriction point; *% EL*, percent egg length; *uni(a)*, unidirectional shift anterior; *comp*, complete retraction; *nr*, not recorded; *na*, not applicable; ++, +, ±, and − indicate vigorous, intermediate, slight, or no detectable cytoplasmic flow.

ter cycle 6 were quite different from fountain streaming. Slow, steady movements of the cytoplasm from the poles to the center were observed in all ten recordings during cycles 1–3, corresponding to slow posterior migration of the energids. In all ten recordings of cycles 7–9, the only cytoplasmic and energid movements were sudden and unidirectional.

We have estimated when in the cell cycle cytoplasmic movements begin. Fountain streaming proceeds for 3–5 min before entry into metaphase; cytoplasm begins to move slowly and slightly before energid movement, and then accelerates. In all cases, streaming ceases as the energids become more difficult to discern, indicating entry into metaphase. To estimate the lengths of the phases of the cell cycle in the early embryo we calculated a mitotic index. Of 339 fixed embryos in cycles 4–8, 26.8% were in interphase, 24.8% were in prophase, 24.5% were in metaphase, 11.8% were in anaphase, and 12.1% were in telophase. Since each preblastoderm cycle is 8–9 min long at 25°C (Rabinowitz, 1941; our unpublished data), we estimate that interphase, prophase, and metaphase take 2 min each. Therefore, fountain streaming begins in interphase, proceeds vigorously during prophase, and ceases during metaphase, after which cytoplasmic flow reverses. This is identical to the phase specificity determined for energid movements during axial expansion (Baker et al., 1993).

We used video tapes made at higher magnification (400×) to follow cytoplasmic movements in more detail. Fig. 2 *F* is a tracing of particles in the cytoplasm as fountain streaming occurs. The trace begins before streaming starts, and particles were followed by marking their positions every minute until the end of streaming. Two details are clear in these tracings: first, particles in the polar peripheral cytoplasm move slowly, if at all, compared to particles in the peripheral cytoplasm near the middle of the embryo. Second, particles in the deep cytoplasm that flow into the polar region circulate and join the flow of the peripheral cytoplasm.

Energids Converge as They Extend

If cytoplasmic flow moves energids during axial expansion, inflow of cytoplasm at the constriction point should carry lateral energids deeper into the embryo. We verified this by tracing the motions of the energids in 12 expansion movements (cycle 4 or 5) from 9 time-lapse recordings. We measured vectors for 70 energids (Fig. 2 *G*); between 4 and 9 energids can be followed during each expansion. 27 are either anterior- or posterior-most of the visible energids, and 43 are lateral or anterior- or posterior-lateral as shown in Fig. 2 *G*. The vectors trace energids from their stationary positions at the beginning of the cell cycle until just before entry into metaphase. All but one of the lateral energid vectors in Fig. 2 *G* move toward the midline. Lateral energids migrate inward on the order of 10 μm during each extension; the greatest inward length was ~25 μm.

Regardless of the mechanism, any movement of a nucleus in an egg of fixed volume necessitates an opposite movement of an equal volume of material. This cannot be the reason for the cytoplasmic streaming we observe. The streaming we observe is of far greater magnitude than volumetric exclusion would require. Furthermore, throughout preblastoderm development energids move with the cytoplasm rather than against it. Thus, we observe dramatic streaming motions of cytoplasm accompanying nuclear migration, rather than nuclei pushing their way through an essentially fixed cytoplasm. By contrast, cortically migrating nuclei in later cycles presumably displace cytoplasm, and cortical migration is not accompanied by cytoplasmic streaming in the direction of nuclear movement. These observations lead us to conclude that fountain streaming of the egg cytoplasm moves the nuclei during axial expansion.

Microfilaments Form an Extensive Network throughout the Embryo

We have characterized the distribution of F-actin in whole-mounted embryos fixed during axial expansion. We distinguish four configurations of F-actin: a dense cortical layer, a network of fibers that extends throughout the embryo, clusters of F-actin around the nuclei, and a "central domain" between the nuclei (Fig. 3). The central domain is a concentration of F-actin found in the center of the nuclear ellipsoid (Hatanaka and Okada, 1991; *arrow* in Fig. 3). Fig. 4 illus-

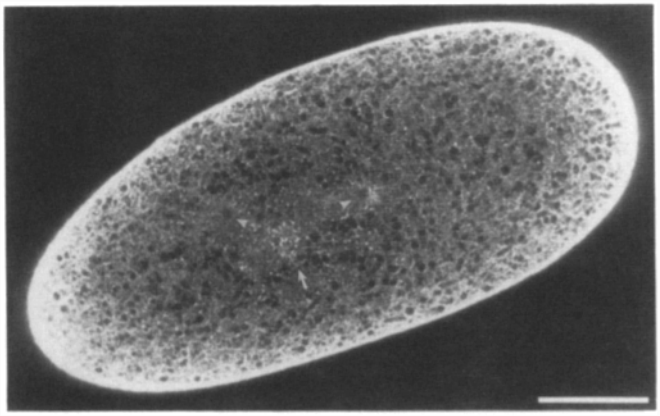

Figure 3. Distribution of F-actin during axial expansion. Anterior is to the left. Frontal confocal optical section from an embryo in late interphase cycle 5 stained with BFL-phl. Beneath the bright cortical layer of F-actin is a dense network of fibers and diffuse material interspersed with granules. The positions of nuclei are indicated by arrowheads; other dark circles are yolk spheres. The posterior nucleus is associated with a cluster of F-actin called an actin cap. The central domain is indicated by an arrow. Note that the network is brighter and appears more fibrous nearer the periphery of the embryo than in the center. Bar, 50 μm.

trates F-actin configurations at high magnification; Fig. 4 *A* illustrates all four configurations in a single image. We have not observed any changes in the form or distribution of the cortical F-actin layer with either cycle phase or number throughout preblastoderm development. It is made up of intensely staining F-actin granules (Fig. 4 *B*), with no connections visible between adjacent granules. In contrast to the cortical layer, the fibrous network beneath it incorporates both fibers and diffusely stained material, interspersed with yolk granules (Fig. 4 *C*). We assume that the fibers represent bundles of microfilaments variable in thickness and length, and that diffuse staining represents a mesh of individual microfilaments. Small F-actin granules are often found within the network, especially near the cortex. As illustrated in Figs. 3 and 4 *A* and below, the network is not uniform throughout the embryo; the region of cytoplasm near the cortex is much more brightly stained by phl than the region around the nuclei. In addition, the density of fibers in the network is much higher near the cortex than around the nuclei. This phenomenon is specific to interphase and prophase, as described in more detail below. The central domain is composed of both F-actin granules and short fibers (Fig. 4 *D*). Fibers occasionally appear to radiate from granules within the central domain, but fibers in the central domain are rare and shorter than in the fibrous network. The central domain is most prominent during interphase and prophase from cycle 4 through 9. Finally, Fig. 4 *F* illustrates "actin caps" around nuclei from an embryo in interphase 7. By cycle 7, caps are obvious around all nuclei throughout the cell cycle.

Cell Cycle–coordinated Reorganization of the Actin Caps

We describe first the changes the actin caps undergo during the cell cycle. Fig. 5 shows actin caps in the different phases of cycles 5 and 6. During interphase and prophase the caps of lateral nuclei are apically oriented (that is, toward the cortex; Figs. 4 *F* and 5 *A*). The cap is located on the poleward side of the anterior- and posterior-most nuclei (Fig. 5, *B*, *F*, *G*, and *H*). Caps appear similar in shape in interphase and prophase, but are less prominent in prophase. In fact, in prophase of cycles 4 and 5 (but not 6; see Fig. 4 *A*) actin caps are only seen around the posterior- and anterior-most nuclei, and the cytoplasm around the lateral nuclei is only dimly stained relative to the fibrous network (Fig. 5 *G*). The posterior-most nuclei have much stronger caps compared to other nuclei during cycles 4–6 (compare Fig. 5, *A* and *B*). The anterior-most nuclei have weaker caps, and lateral nuclei have the weakest caps. The non-equivalence of actin caps during cycles 4–6 is evident in all phases except metaphase, when all caps are equivalent. Fig. 5, *D* and *E* are a lateral telophase pair and a posterior pair, respectively, from the same cycle 5 embryo. The posterior pair has a much more extensive array of fibers at each pole than the lateral pair. It is also obvious in Fig. 5 *E* that the posterior daughter has a more extensive actin cap than the anterior daughter.

Because of their location relative to the nuclei, actin caps appear to be organized around the microtubule-organizing center (MTOC). In metaphase, anaphase, and telophase the positions of the spindle poles are inferred from the alignment of chromosomes or daughter nuclei, and in interphase the MTOC is apical to each nucleus (Baker et al., 1994; see Fig. 6 below). In metaphase the actin caps are very small, smoothly stained foci at the spindle poles (Fig. 5 *C*). During anaphase and telophase the foci are larger than in metaphase, and fibers radiate from them into the surrounding fibrous network and along the sides of the spindle (Fig. 5, *D* and *E*). During interphase, many long, thin fibers are still visible running between nuclei and toward the central domain (Figs. 4 *F* and 5 *A*), and granules accumulate in the more prominent caps (Fig. 5, *B* and *F*). Although caps include fibers during prophase, they are shorter, and late in prophase there are few connections between adjacent nuclei or between nuclei and the central domain (Figs. 4 *A* and 5, *G* and *H*). During interphase and prophase, the foci of smoothly stained material in each cap are less obvious. Thus, a focus of smoothly staining F-actin persists at each MTOC throughout the cell cycle, and the array of F-actin fibers that networks the nuclei and the central domain is developed during anaphase and telophase. We suggest that the fiber array disassembles into the granules that cluster in the actin cap during late interphase and prophase, and that the granules either dissolve or disperse from the nucleus by the beginning of metaphase.

The Central Domain

The central domain reflects cell cycle–coordinated reorganization of F-actin similar to what we observe in the actin caps above. We have examined over two hundred embryos between cycles 4 and 8, and noted the position and prominence of the central domain. It is most prominent during late interphase and prophase (compare Fig. 7, *A* and *B*, below, to 7 *C*) and is always located slightly anterior of center in the nuclear ellipsoid. The energids at the anterior-most and posterior-most positions in the ellipsoid migrate most, and the posterior energids move further posteriorly than the anterior energids move anteriorly (Fig. 2 *G*). Thus, the central domain colocalizes with nuclei which move the least, the lateral nuclei. During cycle 4, the central domain is a sphere

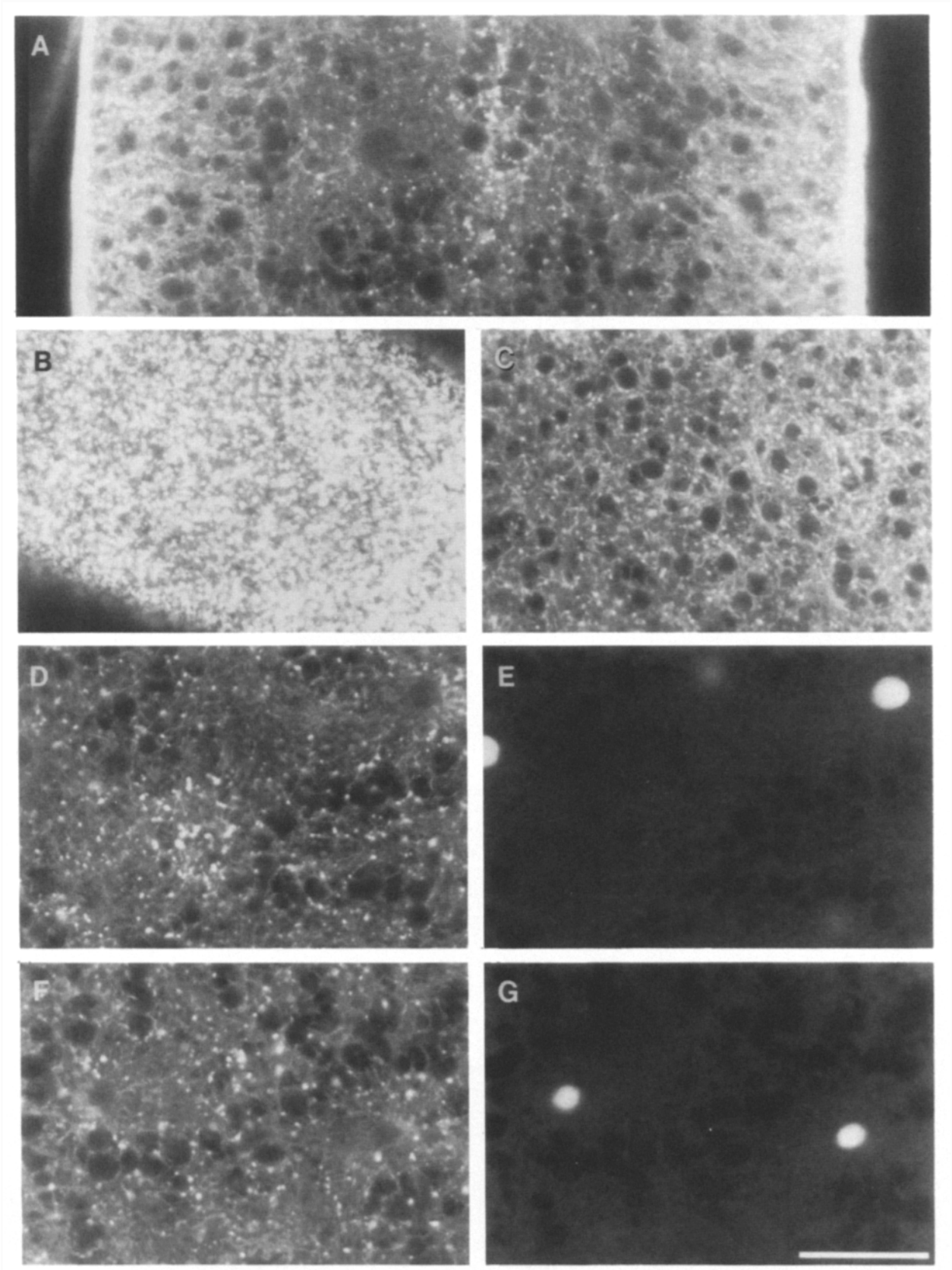

Figure 4. Detail of different F-actin configurations. F-actin (BFL-phl; *A*, *B*, *C*, *D*, and *F*) and histone (*E* and *G*). (*A*) Prophase of cycle 6, saggital plane. Note how the consistency of the fibrous network changes from the periphery to the center of the embryo. Near the surface the network is dense and includes many long fibers; deeper in the embryo, there are fewer fibers and most of these are quite short. In the very center is the central domain, which contains very few fibers. *B* is a projection of three grazing sections of an embryo in interphase 5. Although it appears to be a smooth layer in medial sections, the cortical layer is made up of distinct F-actin granules which vary considerably in size. (*C*) The fibrous network. The single section was collected ~15 μm beneath the surface of the embryo. Notice how fibers wrap tightly around yolk platelets, sometimes encircling them. F-actin (*D*) and histone (*E*); single section of the central domain from late interphase 5. This was collected from the same embryo and at the same level as shown in Fig. 3, but at higher resolution. In several instances in this image a fiber can be seen apparently radiating from a granule. F-actin (*F*) and histone (*G*); actin caps in early interphase 7 (single section). Actin caps are apically oriented, with many long fine fibers projecting toward the center. Bar, 20 μm.

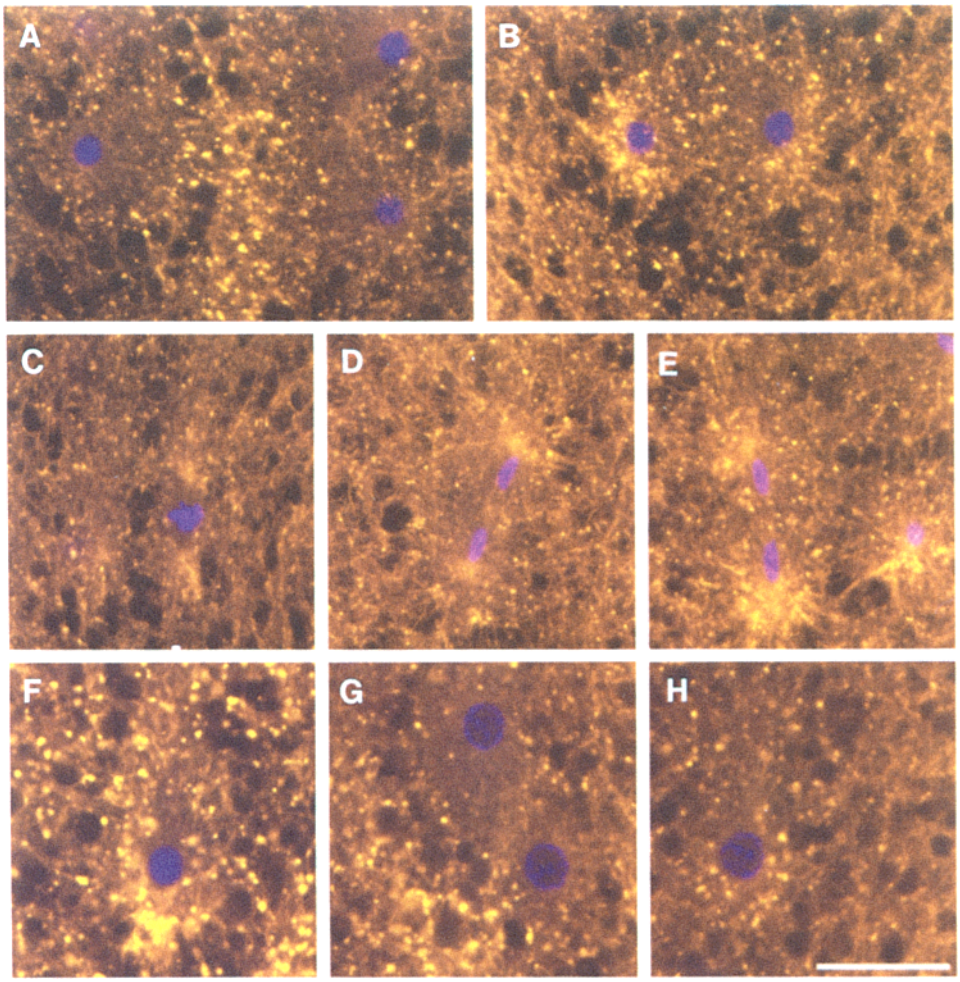

Figure 5. Actin caps change with the cell cycle. Images shown are from embryos fixed at different stages of cycles 5 and 6. *A–E* are projections of three consecutive sections, *F–H* are single sections. In all, F-actin (BFL-phl) is false-colored orange and histone is blue; anterior is toward the top of the page. (*A* and *B*) Interphase 6, lateral nuclei (*A*), and posterior nuclei (*B*). Actin caps are present but not prominent around the lateral nuclei, and consist principally of long fine fibers that project toward the central domain. The posterior nuclei are associated with large prominent clouds of granules and fibers, however. (*C*) Metaphase 5. At each spindle pole there is an irregularly shaped accumulation of F-actin. All actin caps are equivalent in metaphase; *C* shows the posterior-most nucleus. As reflected in this image, granules are much scarcer and less obvious in metaphase (unpublished data). (*D* and *E*) Telophase 5, lateral nuclei (*D*), and posterior nuclei (*E*). In lateral nuclei, the caps at the spindle poles have grown slightly, and a few fibers extend outward. Around the posterior-most nuclei, however, the actin caps have grown enormously, including both rather thick fibers and large granules. Unlike actin caps in the syncytial blastoderm (Yasuda et al., 1991), we do not see accumulation of F-actin at the metaphase plate. (*F*) Late interphase 5, the posterior-most nucleus. In interphase, the bright posterior cap includes mostly granules with a few fibers radiating from them (compare *B* and *F* to *E*). (*G* and *H*) Prophase 5, lateral nuclei (*G*), and posterior nucleus (*H*). Comparing *H* to *F*, the granules in the cap in prophase are smaller, the fibers are virtually gone, and the overall amount of F-actin is less. We infer from this series that actin caps form and break down during each cell cycle. They seem to "nucleate" around each spindle pole in metaphase, grow during anaphase and telophase, and disperse during interphase and prophase. Note that the amount of F-actin incorporated into the cap is correlated with the amount of movement that a nucleus undergoes during extension (see Fig. 2 *G*). Posterior nuclei move the most, and they have the largest caps. Anterior nuclei move somewhat less, and have less prominent caps. Lateral nuclei move the least and have the faintest caps of all. Bar, 20 μm.

roughly 10 μm in diameter (Fig. 6 *A*). During the next cycle, it increases slightly in diameter (Fig. 6 *D*). In cycle 6 (not shown), it becomes elongated, and lies between a third to a half of the nuclei, always in the middle of the nuclear ellipsoid but slightly anterior, as in cycle 5. We do not see the central domain disappear after cycle 6 as reported by Hatanaka and Okada (1991); we observe it at least through cycle 9 during late interphase and prophase. During cycle 7 it is a thin streak running the length of the nuclear ellipsoid, and in cycles 8 and 9 it is broader (not shown); the central domain thus increases in size as the nuclei increase in number.

During interphase, microtubules form an extensive network in which short microtubules radiate toward the cortex and long microtubules radiate inward (Baker et al., 1993; Fig. 6, *B*, *E*, and *H*). Double labeling for F-actin and tubulin shows that during interphase of cycles 4–9, the central domain always arises exactly where the distal ends of microtubules from different nuclei intersect (Fig. 6). Granules do not accumulate in areas where microtubules simply coextend but only in regions of overlap between the distal ends of microtubules radiating from multiple nuclei (Fig. 6, *D–I*). Fig. 6, *G–I* are from an unusual interphase 5 embryo in which two central domains were present. In this case, both central domains colocalize with two independent regions of microtubule overlap.

Disassembly of the Actin Cytoskeleton during Interphase and Prophase

In Fig. 3 there appears to be less F-actin in the fibrous network around the nuclear ellipsoid than near the cortex. This

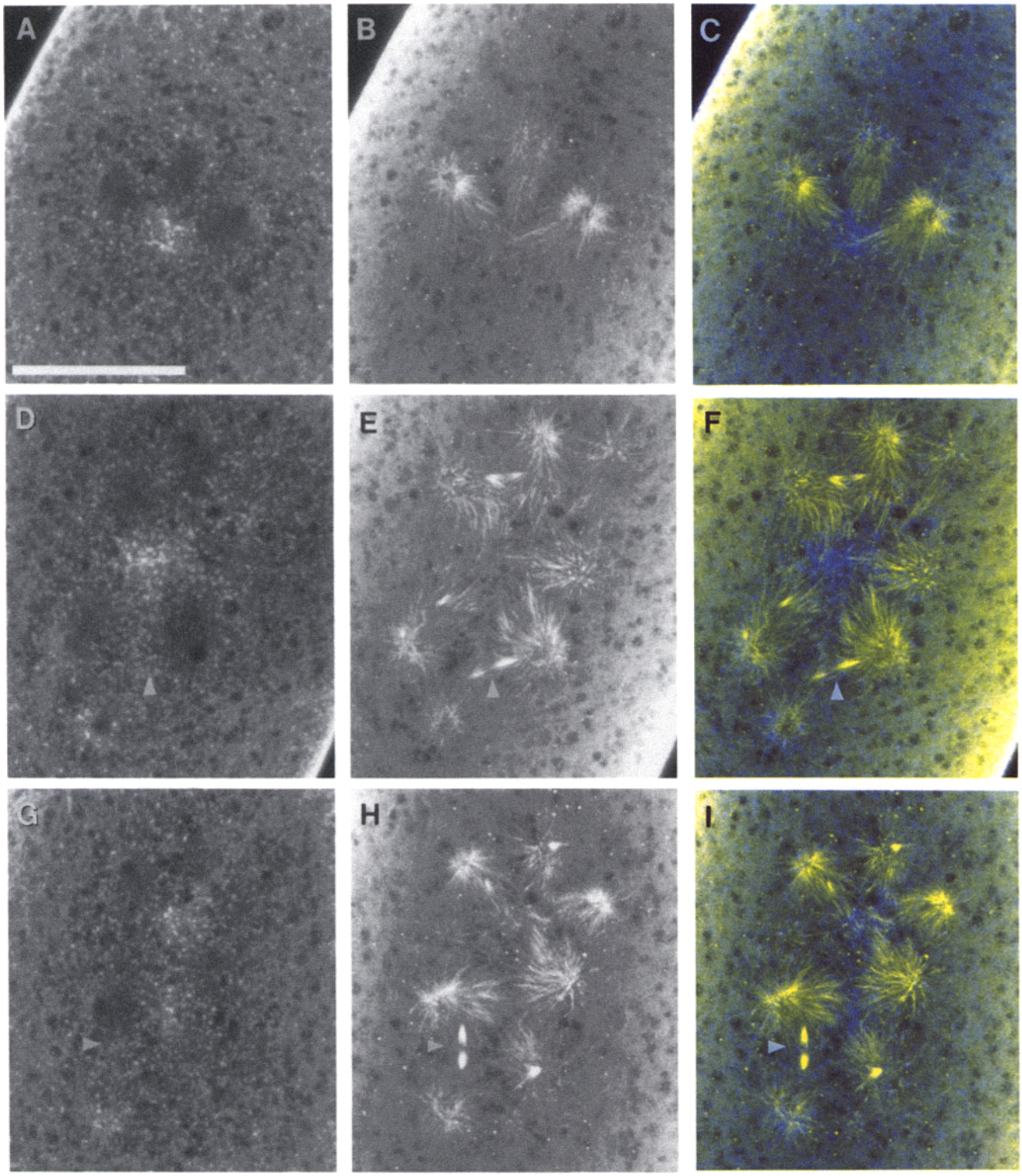

Figure 6. The central domain collects at the intersection between microtubule distal ends. All images are projections of five consecutive sections; anterior is up. F-actin (BR-phl; *A*, *D*, and *G*), tubulin (*B*, *E*, and *H*), and false-colored merge (*C*, *F*, and *I*) with actin in blue and tubulin in yellow. All embryos are in late interphase, as judged by the microtubule configuration (Baker et al., 1993). (*A–C*) Cycle 4. Microtubules from three independent, non-sister nuclei are visible in this plane. These three sets of inwardly directed microtubules all converge with their distal ends at the location of the central domain. Sections through this embryo show that long microtubules radiate from 4 of the other 5 nuclei in this embryo (not seen in this projection) toward the position of the central domain; microtubules emanating from the most posterior nucleus (not seen) did not reach the central domain. (*D–F* and *G–I*) Cycle 5. In each case, granules accumulate in the overlap region between astral microtubules. In most embryos, there exists a single overlap region and a single central domain. The embryo shown in *G–I* possessed two such regions of microtubule overlap and consequently two central domains. F-actin does not visibly accumulate between the two halves of the midbody (*arrowheads* in *D–I*), or at the metaphase plate (see Fig. 5 *C*). Bar, 50 μm.

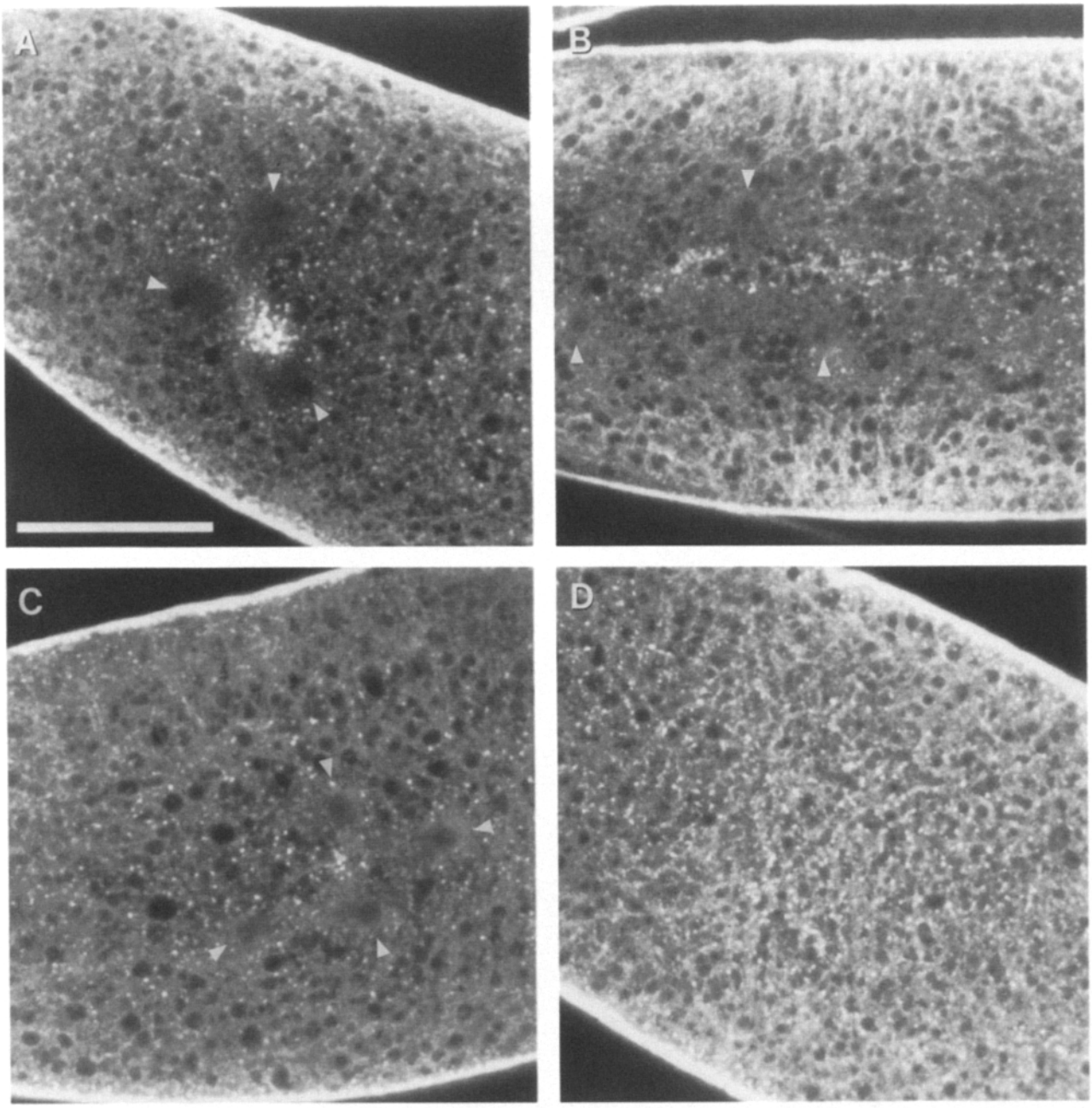

Figure 7. Melting of the fibrous network around the nuclei. All images are single medial sections of BFL-phl stained embryos; anterior is left. (*A*) Prophase 4. In this plane, three nuclei (*arrowheads*) encircle the central domain. The intensity of signal is much reduced in the nuclear region compared to the peripheral region (compare to *C*). In regions of the embryo not yet populated by nuclei the fibrous network is evenly labeled. (*B*) Prophase 6. Nuclei (*arrowheads*) populate a clearly demarcated region of reduced labeling with an elongated central domain between them. Melting is more obvious in cycle 6 than in cycle 4 because of the sharp demarcation between regions. The degree of melting is similar in all of cycles 4–6. (*C*) Metaphase 4. Four nuclei are visible in this plane (*arrowheads*). In contrast to *A* and *B*, labeling is even throughout the embryo. (*D*) Unfertilized egg. As in metaphase embryos, labeling is even throughout the embryo. We have fortuitously observed more than 10 unfertilized eggs in collections of wild-type embryos stained for F-actin, and all look identical to *D*. Bar, 50 μm.

is obvious during interphase and prophase, but not during metaphase (compare Fig. 7, *A* and *B* to *C*). In prophase 6, the nuclei populate a clearly demarcated internal zone in which the intensity of phalloidin labeling is greatly reduced (Fig. 7 *B*). Unfertilized eggs contain a fibrous network of apparently normal architecture, but do not exhibit a region of reduced staining (Fig. 7 *D*). These observations and those above concerning the central domain and cell-cycle–coordinated reorganization of actin caps suggest that the fibrous network loosens around the nuclear ellipsoid relative to the peripheral region during interphase and prophase.

To demonstrate a correlation between cell cycle phase and

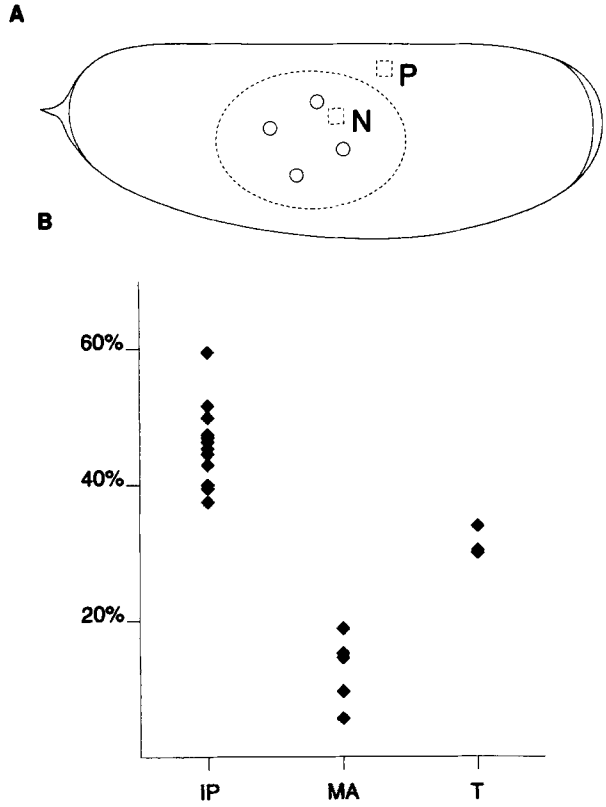

Figure 8. Diminished F-actin signal intensity in the nuclear region during interphase and prophase. (*A*) This diagram summarizes our method for measuring disassembly of the fibrous network around the nuclei. We measured and averaged intensity within several square areas of the size shown in the nuclear region (*N*) and the peripheral region (*P*). (*B*) Graph of the signal intensity difference, expressed as a percentage (%) (P-N)/P, between the peripheral network and around the nuclei. *IP*, interphase/prophase; *MA*, metaphase/anaphase; *T*, telophase. Measurements were made from single medial optical sections of 20 embryos in cycle 5 or 6 from a single collection and staining experiment. As described in Materials and Methods, these measurements contain a very significant baseline due to autofluorescence and the presence of yolk spheres, and the shape of the embryo contributes a 5–10% decline in signal between the two regions. If adjusted for these quantities the MA differences change very little but the IP differences are greatly enhanced.

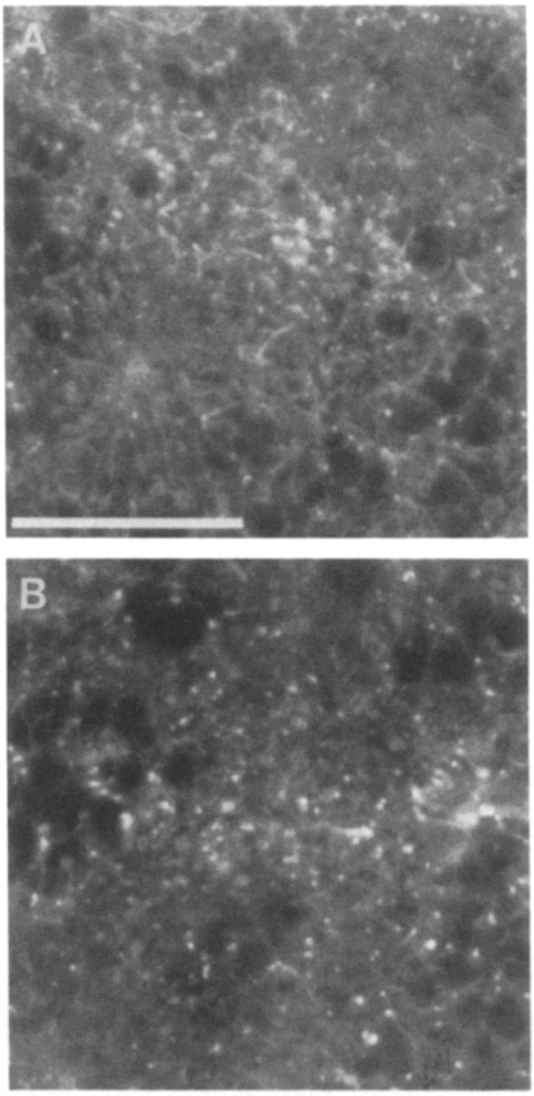

Figure 9. Disappearance of fibers in the nuclear region during interphase and prophase. Both images are single medial-level optical sections at high magnification collected from embryos stained with BFL-phl. (*A*) Metaphase 5. Many short (~5 μm) fibers or fiber segments are visible in this section. (*B*) Prophase 6. This section cuts through the uppermost portion of the central domain. Very few fibers are visible, and the overall staining is also reduced. Bar, 20 μm.

redistribution of F-actin, we have measured the intensity of phalloidin labeling in the peripheral and nuclear region of medial optical sections from a set of 20 embryos in cycles 5 or 6 (Fig. 8 *A*). Since phl labels only F-actin, the level of signal measured is proportional to the quantity of F-actin present in that area. We detect 40–50% less F-actin in the nuclear region relative to the peripheral region in interphase and prophase embryos (Fig. 8 *B*). A 30–35% difference is detected in telophase, and a nominal difference of 5–20% is detected in metaphase and anaphase embryos.

In addition to reduced signal around the nuclear ellipsoid, the nuclear region appears to become depleted of fibers during interphase and prophase (Fig. 4 *A*; compare Fig. 9, *A* and *B*). To test this, we made traces of selected areas from high magnification images of 13 embryos. We then counted the number of fibers visible in each representative area (Table II). In interphase, about twice as many fibers are visible in the peripheral region as in the nuclear region, with one exception in which the chosen regions were not different. In prophase the difference is somewhat greater, ranging between twofold to over fourfold. In metaphase the number of fibers in the two regions are roughly equivalent.

Because the intensity of signal is roughly equivalent in the peripheral regions between embryos of different cell cycle phases (data not shown), we infer that large differences in F-actin concentration reflect disassembly of the fibrous network in the nuclear region. This is supported by counting of fibers, which demonstrates that the nuclear region becomes depleted of this structural element during interphase and prophase. Therefore, we conclude that the fibrous network

Table II. Fibers Become Scarce in the Nuclear Domain during Interphase and Prophase

Phase	P	N	P:N
Inter 5	56	29	1.9
Inter 5	48	23	2.1
Inter 6	64	33	1.9
Inter 6	35	34	1.0
Inter 6	40	16	2.5
Pro 5	57	22	2.6
Pro 5	33	12	2.8
Pro 6	42	21	2.0
Pro 6	52	12	4.3
Pro 6	39	15	2.6
Meta 5	43	46	0.9
Meta 5	47	31	1.5
Meta 5	41	38	1.1

* Each row represents an individual embryo from which two representative areas were selected for tracing. Numbers indicate total number of distinct, traceable fibers in both sampled areas of each region of each embryo (see Materials and Methods).
P, area in peripheral region; *N*, area in nuclear region (see Fig. 8 *A*); *P:N*, ratio of P to N.

is partially disassembled around the nuclei during interphase and prophase, and is reassembled during metaphase.

Effects of Cytoskeletal Inhibitors on Microfilament Configuration

Cytochalasin D (CytD) and phalloidin (phl) both inhibit microfilament function but have opposite effects on actin dynamics. Cytochalasins inhibit polymerization while phl promotes it. Zalokar and Erk (1976) and more recently Hatanaka and Okada (1991) reported that cytochalasin inhibits axial expansion. We have repeated this experiment by injecting CytD into embryos at cycle 4 and fixing them 10 and 30 min after injection. When analyzed on time-lapse video tapes, cytoplasmic movements are inhibited or abnormal within 10 min of CytD injection. We have measured the length of the nuclear ellipsoid in fixed CytD-injected and in buffer-injected embryos to verify that CytD inhibits axial expansion (data not shown). 30 min after CytD injection, staining with phl reveals no fibrous network although buffer-injected embryos appear normal (compare Fig. 10, *A* and *C*). Many CytD-injected embryos have a central domain and a bright layer of F-actin at the cortex (Fig. 10 *C*). We have also examined the effects of phl injection on F-actin distribution and nuclear migration (Fig. 11). On analyzing time-lapse video tapes of injected embryos, we find that high concentrations of phl cause immediate arrest, but that low concentrations affect only the area near the injection. We have fixed and stained embryos 20 min after phl injection and stained with labeled phl. The fibrous network is greatly enhanced in the area of the embryo near the site of injection, though the morphology of the network is unchanged (Fig. 11, *A* and *C*). Nuclei become trapped in the enhanced fibrous network and are unable to migrate or divide, although nuclei elsewhere are able to migrate, divide, and establish a relatively normal arrangement (Fig. 11 *B*).

Baker et al. (1993) reported that injection of cycloheximide (CYH), an inhibitor of protein synthesis, blocks nuclear division and axial expansion, but not cortical migra-

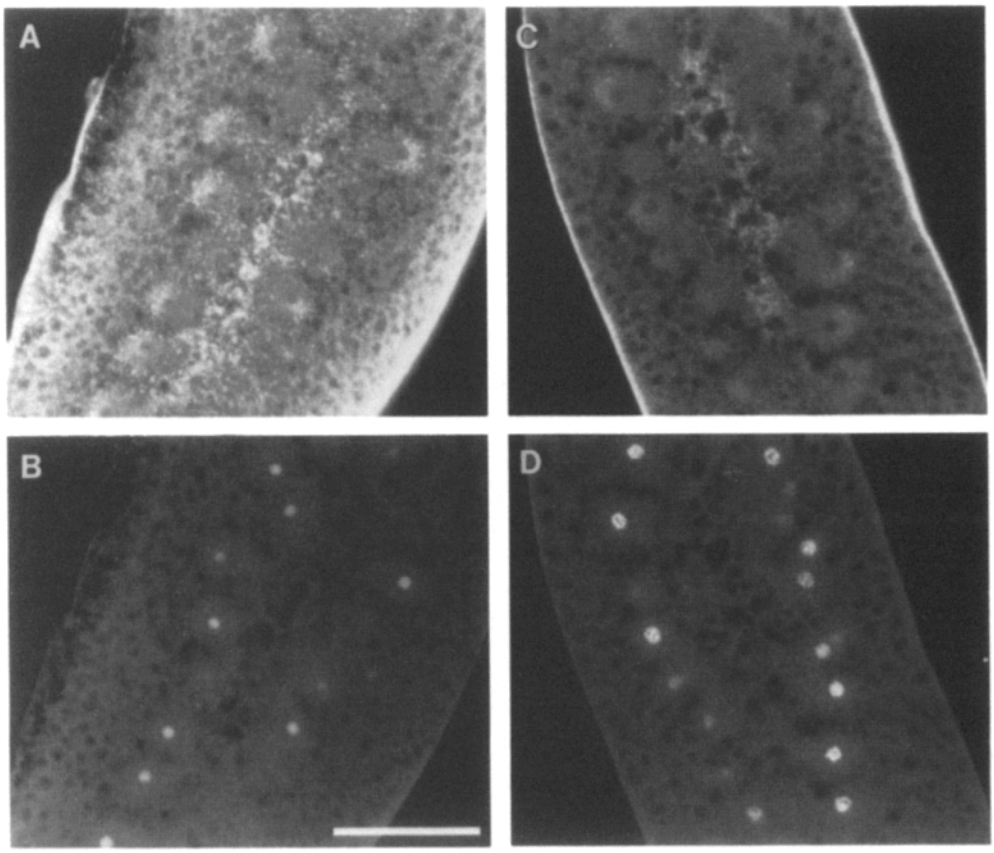

Figure 10. Cytochalasin abolishes the fibrous network. Embryos were injected at 40 min AED, fixed 30 min after injection, and stained with BFL-phl (*A* and *C*) and histone (*B* and *D*); anterior is up. (*A* and *B*) Buffer-injected, interphase 7. F-actin distribution appears normal; the rough surface on one side of the embryo is damaged from mounting. (*C* and *D*) CytD-injected, prophase 7. The fibrous network is gone; staining in the cytoplasm is barely above the background autofluorescence. Cortical layer, central domain, and actin caps are present but reduced. Bar, 50 μm.

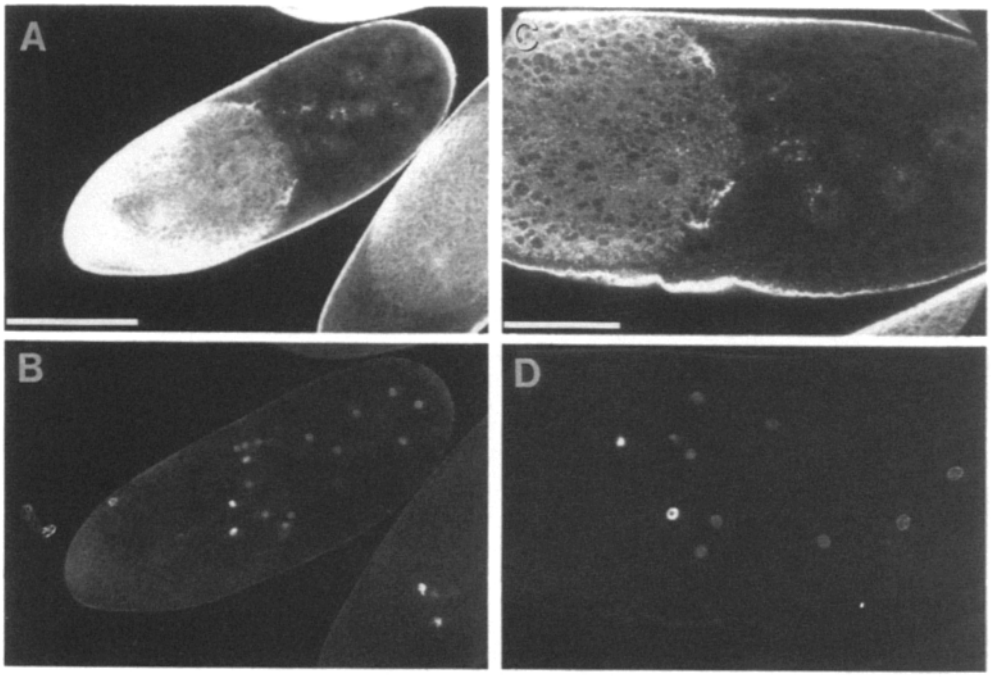

Figure 11. Phalloidin inhibits nuclear migration by enhancing the fibrous network. Embryos were injected 40 min AED with 6 μg/mL phl, fixed 20 min after injection, and double stained with BFL-phl (*A* and *C*) and histone (*B* and *D*); anterior is left. *C* and *D* are higher magnification views of the same embryo shown in *A* and *B*. Bar in *A*, 100 μm; Bar in *C*, 50 μm.

tion. CYH arrests the cell cycle in late interphase (Edgar et al., 1986), and Baker et al. (1993) demonstrated that CYH injection leads to overgrowth of the interphase microtubule network. We repeated this experiment to determine the effect of interphase arrest on the actin cytoskeleton. As with CytD, cytoplasmic movements are inhibited or abnormal after CYH injection. We have injected embryos at cycle 4 with CYH and fixed them 10 and 30 min after injection. 10 min after CYH injection, few fibers are visible in the network, and in many embryos the central domain appears more prominent (data not shown). In embryos fixed 30 min after CYH injection, there is no evidence of the fibrous network. Instead, all the F-actin in the embryo is in the cortical layer or in a giant central domain-like cluster of F-actin granules between the nuclei (Fig. 12, *C* and *D*; compare with buffer-injected control, Fig. 12, *A* and *B*). No fibers are visible after 30 min in CYH-injected embryos. In contrast, buffer-injected control embryos display a dense fibrous network, as in wild-type, uninjected embryos (compare with Figs. 3 and 4 *A*). This experiment indicates a correlation between interphase/prophase of the cell cycle and the reorganization of the actin cytoskeleton by the nuclei; the most parsimonious interpretation is that when the cell cycle remains in interphase/prophase for an extended period, disassembly of the fibrous network proceeds to completion.

Discussion

Foe et al. (1993) presented an elegant explanation for axial expansion in which cortical migration and axial expansion are both caused by microtubule-mediated mutual repulsion. They proposed that actin "contributes to a cytogel, whose stiffness is greatest near the actin-rich cortex and least near the embryo's core." Thus, mutual repulsion between the nuclei should result first in formation of an ellipsoid, and then in isometric migration to the cortex. This hypothesis is made untenable by recent observations; cortical migration occurs in telophase and interphase when microtubules are long, but axial expansion occurs predominantly during prophase when microtubules are short relative to the distance between neighboring nuclei (Baker et al., 1993).

As anticipated by Foe et al. (1993), actin contributes to a "cytogel" whose stiffness is greatest near the periphery of the embryo. Based on the results of phl injection, the network is stiff and resists movement of nuclei and cytoplasm. Further, we assert that a decrease in the intensity of F-actin staining and in the abundance of fibers reflects partial solation of the cytogel, although this statement requires verification by direct measurement of viscosity. Foe et al. (1993) envisioned a looser region of the cytogel matching the shape of the embryo, and that the nuclear configuration would match the shape of this easier-to-penetrate region only at the end of axial expansion. However, we find instead that solation correlates with cell cycle phase, and the shape of the solated region changes, always matching the nuclear domain.

Three drug treatments have different effects on the distribution of F-actin: CytD inhibits actin polymerization and consequently the fibrous network disappears and axial expansion does not occur, phl promotes actin polymerization and therefore nuclei become trapped in a denser network, and CYH, by arresting the cell cycle in late interphase, leads indirectly to the complete conversion of the fibrous network to granules of F-actin. Either CytD or CYH injection abolishes the fibrous network and inhibits both fountain streaming and axial expansion. Thus, the fibrous network does not act simply to resist passively the movement of nuclei. If this were the case, we might expect these treatments to facilitate expansion. Instead, these drugs inhibit fountain streaming by destroying the network; thus, the network does more than transduce cytoplasmic movements to the nuclei. It must be necessary for streaming.

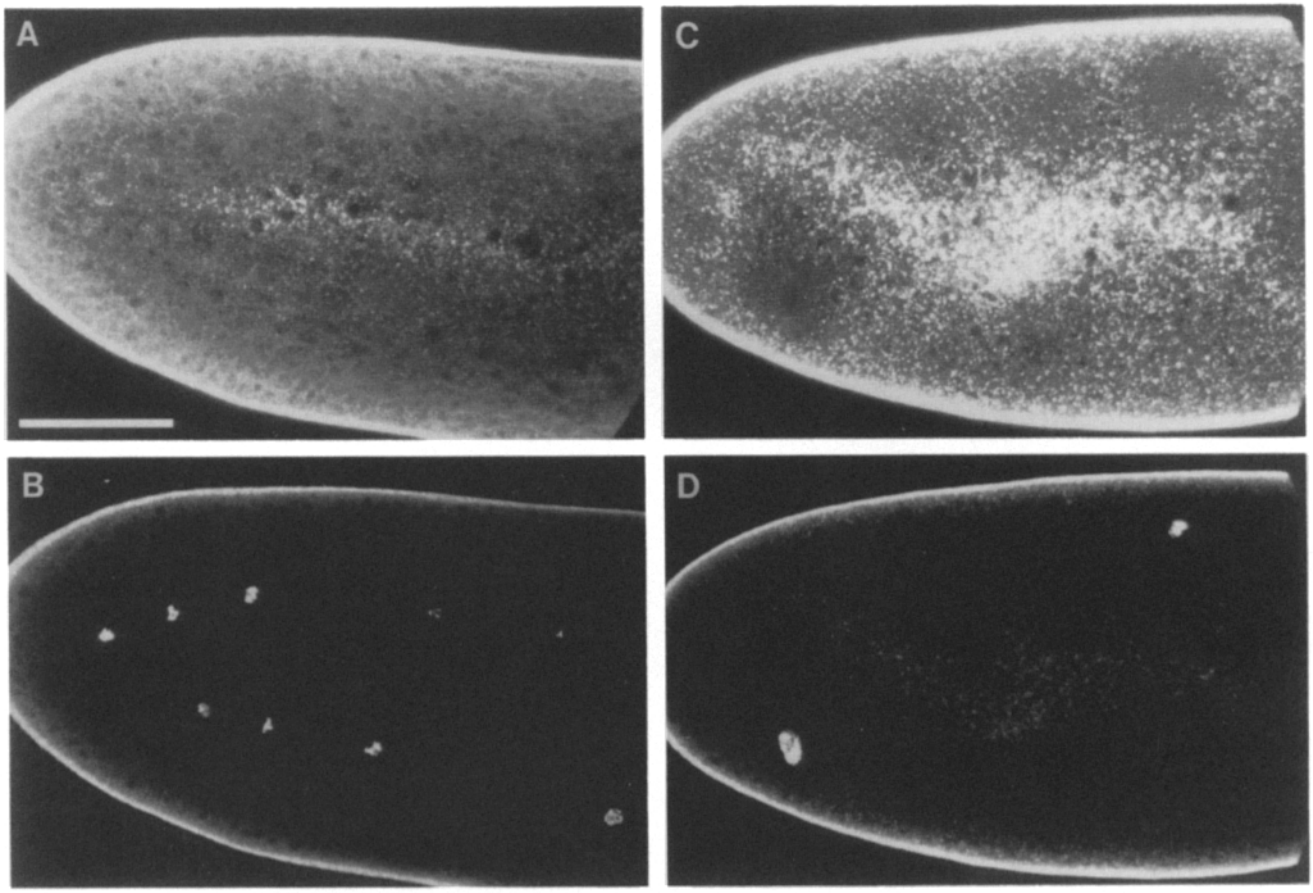

Figure 12. Cycloheximide induces complete reorganization of the fibrous network to central domain. Embryos were injected at 40 min AED, fixed 30 min after injection, and stained with FITC-phl (*A* and *C*) and histone (*B* and *D*); anterior is left. (*A* and *B*) Buffer-injected, late prophase/metaphase 7. F-actin distribution appears normal. (*C* and *D*) CYH-injected. No network is visible; all F-actin is in either the cortical layer or in a huge collection of granules between the nuclei. Bar, 50 μm.

Models for Microfilament-dependent Cytoplasmic Movement

Fountain streaming is a common phenomenon in large cells such as giant amoebae and some embryos (Counce, 1973; Allen, 1973; Hird and White, 1993). Two general hypotheses have been advanced that explain how the actin cytoskeleton causes such cytoplasmic movements. The first involves contraction and redistribution of cytoskeletal units in the cortex, and originated with the analysis of cytokinesis (White and Borisy, 1983). Hird and White (1993) invoked cortical contraction to interpret their observations on cortical flow, pseudocleavage, and cytokinesis in *Caenorhabditis elegans* embryos. These authors observed that pseudocleavage and cytokinesis are accompanied by cytoplasmic streaming similar to the flow we report here during axial expansion in *Drosophila*. They propose that relaxation of the cortical cytoskeleton at the poles combined with contraction and transport of the contracting elements toward the equator directs the formation of a contractile ring-like structure.

The cortical contraction hypothesis explains the data in *C. elegans*, but does not explain our observations on axial expansion. We have not observed accumulation of F-actin near the constriction point as one would expect from such a mechanism. Furthermore, there is no infolding of the cortex in *Drosophila* as there is during cytokinesis or pseudocleavage in *C. elegans*. Also, it is difficult to imagine how stimulation of fountain streaming might be coupled to the position of the nuclear domain (see below); cortical contraction models rely on the influence of the asters on the cortical cytoskeleton (White and Borisy, 1983), but no such interaction seems possible here.

The second hypothesis is derived from studies on the extension of the pseudopod of amoeboid cells (Allen, 1973). During extension of the pseudopod, a fountain of partially solated deep cytoplasm (endoplasm) streams toward the pseudopod tip through a tube of gelled material (ectoplasm). In Allen's frontal contraction model, fountain streaming occurs because the endoplasmic cytoskeleton is anchored near the tip and contracts toward it. The endoplasmic cytoskeleton is composed principally of long contractile strands of actin and myosin (Taylor et al., 1973), and one formulation of the pseudopod supposes that these actin/myosin strands compile into the ectoplasmic tube as they reach the tip, pulling endoplasm tipward by viscous drag (Odell, 1977). At the same time tail contractions, resulting from partial solation of ectoplasm and recruitment into endoplasm, might propel more material into the pseudopod (Taylor and Fechheimer, 1982). This model thus proposes a gradient of gelation and

solation in the pseudopod which directs contraction of actin/myosin strands.

Based on the characteristics of isolated amoeba cytoplasm and reconstituted actin/myosin networks, Taylor and coworkers developed the solation-contraction coupling hypothesis (Taylor and Fechheimer, 1982). When actin filaments bind cross-linking and motor proteins, they will form a gel that contracts. If the gel is anchored, contraction is limited because cross-links eventually restrain further contraction. The basis of the solation-contraction coupling hypothesis is simple: Since contractile actin/myosin gels are limited by their cross-links in the extent to which they may contract, then as a contractile gel begins to solate, it will be induced to contract further. The hypothesis postulates that "a weakened gel cannot resist contraction, but can transmit forces of contraction through its remaining structure," and that "cytoplasmic contraction can be induced by localized decreases in gel structure" (Kolega et al., 1991). Janson et al. (1991) demonstrated that an in vitro reconstituted gel of actin, myosin, and filamin exhibits fountain streaming in response to localized application of cytochalasin. Thus, melting a contractile gel at one end while the other end remains intact and anchored to a rigid support results in contraction of all the gel toward the anchored site and away from the melted site (see Fig. 13 *A*).

Actin in the Preblastoderm Embryo

In the preblastoderm embryo, changes in the appearance of the fibrous network correlate with both cytoplasmic and nuclear movement. During metaphase and anaphase, when no movement occurs, the fibrous network is uniform throughout the embryo. During interphase and prophase, when the cytoplasm flows and nuclei migrate, the actin network in the nuclear region partially disassembles, suggesting that solation-contraction coupling within the network causes fountain streaming. The morphology of the actin cytoskeleton also may reflect solation-induced contraction. Diffusely staining material may be a dense meshwork of individual microfilaments. Fibers are almost certainly bundles of microfilaments, and bundling might result from contraction of a dense meshwork. This result was observed by electron microscopic examination of in vitro reconstituted actin/myosin/gelsolin or actin/myosin/actinin gels induced to contract by calcium addition (Janson and Taylor, 1993). In addition, antibodies to nonmuscle myosin label the region of cytoplasm in which the fibrous network is found (Young et al., 1991; our unpublished observations). Therefore, the morphology of the fibrous network suggests it is actively contractile.

The central domain may also reflect solation-induced contraction. Although we have not yet characterized the F-actin granules ultrastructurally, they may be equivalent to previously described structures. F-actin granules are very prominent in the cortex of *C. elegans* embryos (Strome, 1986) and in the cortex and deep cytoplasm of eggs of *Boltenia*, an ascidian (unpublished observations). F-actin granules also arise during microfilament disassembly in tissue culture cells treated with cytochalasin (see for example Toyama and Toyama, 1988). Most convincingly, Schliwa (1982) showed using high-voltage EM that cytochalasin induces severing of cellular actin networks, and that network fragments subsequently contract in an ATP-dependent manner into knots of short filaments. The granules we observe in the central do-

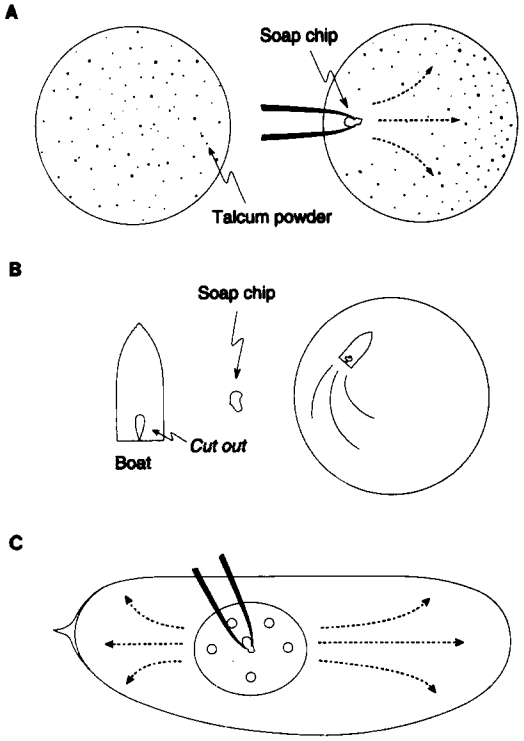

Figure 13. A working hypothesis for axial expansion. The principles behind our hypothesis are illustrated first by analogy. *A* and *B* are two simple demonstrations of directional flow caused by local disruption of tension within a network. The network in both cases is the surface of still water, and the "solating agent" is soap. (*A*) Fill a clean, rinsed pan with cold water and allow to stand until perfectly still. Gently sprinkle talcum powder on the water; these flakes allow one to observe the motion of the surface. Wet a small chip of soap under the tap, and then apply it to one edge of the dish as shown. The talcum flakes will move away from the soap. This is so because the soap locally decreases surface tension as it dissolves; the surface film then "contracts" in the direction of increasing tension. Note the similarity of this demonstration to the results of Janson et al. (1991). (*B*) One may cause a small boat to move using the same principle. Cut from wetable but stiff paper (such as mounting board) a small boat in the shape shown; cut a notch in the stern. Place a chip of soap in the notch, and gently place the boat on the surface of still water. The boat will move forward. Again, the soap is locally decreasing tension within the surface film. The boat surfs along a gradient of tension that it continuously produces beneath itself. (*C*) Our hypothesis for axial expansion involves a tensile network of actin (analogous to the surface film of water) and a locally applied solating agent (analogous to the chip of soap). The solating agent is applied to the network in the region occupied by the nuclei, and consequently the network is induced to contract away from the site of solation. How are the nuclei moved by the resulting contraction? The nuclei or something to which they are attached (the asters?) may interact directly with the contracting actin network, thus "surfing" along the tension gradient like the boat in *B*. Alternatively, the nuclei may not interact directly with the contracting network. Pulling the network through the cytoplasm will result in viscous drag in the direction of the contraction, and the resulting bulk flow could move the nuclei. The demonstrations in *A* and *B* are derived from UNESCO (1958).

main, actin caps, and dispersed throughout the fibrous network may therefore represent super-contracted fragments of the fibrous network.

How Do Nuclei Reorganize the Actin Cytoskeleton?

The solated region is always the domain occupied by the nuclei. Unfertilized eggs do not develop a solated region. Throughout cycles 4 through 9, the solated region matches the nuclear domain, and it enlarges with each successive cycle. In cycles 8 and 9, the fibrous network is reduced to a 10–20-μm layer under the cortex. By the time nuclei have reached the cortex the network is no longer present. Thus, the nuclei continually reorganize the actin cytoskeleton as they encounter it.

The activity associated with the nuclei induces disassembly of the actin cytoskeleton during interphase and prophase, and collects fragments of the network (granules) in the central domain. Double labeling for microtubules and F-actin suggests a role for the aster. Foe et al. (1993) speculate, largely in light of observations on blastoderm-stage embryos, that F-actin intrinsically binds to microtubules and moves toward the plus ends. We have shown that in the preblastoderm embryo, F-actin granules accumulate wherever the distal ends of microtubules intersect. We have not defined the orientation of microtubules in the asters, but is is likely that the plus ends are distal to the nuclei, and so our observations suggest directional transport of F-actin along microtubules as proposed by Foe et al. (1993).

The aster itself could be involved in solation of the actin network. Directional transport of actin toward the distal ends of microtubules would deplete actin around the nuclei, eventually ripping the network. Another hypothesis is that localized calcium release could cause local solation. Calcium activates myosin contractility and stimulates proteins that sever microfilaments, while it inhibits some that contribute to networking (Stossel, 1993), and one formulated theory for solation-induced contraction begins with local release of calcium (Oster and Odell, 1984).

A Working Hypothesis of Axial Expansion

As mentioned above, Janson et al. (1991) demonstrated fountain streaming in an in vitro reconstituted gel in response to local solation; we propose that the same process drives axial expansion in *Drosophila* (Fig. 13). If solation initiated in the exact center of such a gel, as long as the gel's edges were anchored the tendency would be for the unsolated portion of the gel to contract everywhere away from the solated region. We represent the *Drosophila* embryo as if the fibrous network were a similar actin-based gel including cross-linking proteins and myosin. Localized solation would stimulate contraction of the remaining gel. We assume that any given region of the gel has an equivalent contractile tendency, and that the gel is anchored to the cortex. We further assume that pulling the network through the cytoplasm results in bulk flow in the direction of contraction due to viscous drag (Odell, 1977).

We account for the bidirectional fountain pattern by considering the shape of the embryo, the network, and the changing shape of the solated region. The speed of contraction along any radius will be proportional to the volume of gel between the solated region and the cortex, where the gel is attached. Speed of contraction would also be proportional to the size of the solated region and to the degree of solation, since these relate to the amount of tension released. If the region of solation were spherical or slightly ellipsoidal (not yet matching the shape of the cortex) and positioned in the middle of the embryo (Fig. 13 *C*), deep cytoplasm would be pulled most rapidly toward each pole since the greatest expanse of contractile gel is between the poles and the solated region. The need for circulatory flow would dominate over the tendency of the lateral gel to pull material toward the lateral cortex. Peripheral material would be forced by the poleward rush of deep cytoplasm to move toward the middle and flow inward, where it would push the lateral energids deeper into the embryo. The contractile gel reassembles in metaphase; this sets the embryo up to contract again and restrains the nuclei in an extended conformation.

The two parameters that govern the rate of contraction of the gel along any given radius oppose each other. During normal development, as the number of nuclei increases so does the size of the solated region, but at the same time the amount of gel between the solated region and the cortex lessens. Thus, during early mitoses, solation around a few nuclei may not be sufficient to stimulate observable contraction. Only at cycle 4 does axial expansion begin, with mild fountain streaming. Vigorous streaming accompanies cycles 5 and 6; thus, more nuclei and more solation results in more cytoplasmic movement. Later cycles, when the boundary of the solated region matches the cortex, are characterized by irregular shifts. This would be expected if phase specific solation continued, but with only subtle differences to provide directionality to the contractions.

Our hypothesis accounts for the fact that the nuclei comprise of self-centering array. In normal development, axial expansion establishes an ellipsoid of nuclei arranged equidistant from the cortex. The nuclei begin axial expansion asymmetrically placed, with nuclei closer to the anterior pole, and closer to the lateral cortex than to either pole. In agreement with our hypothesis, we noted that the posterior energids migrate faster than the anterior energids. Also, the nuclear array will recenter if pushed to one end of the embryo by an injection needle (unpublished observations). Our model for axial expansion accounts for self-centering behavior by proposing that the amount of a contractile network between the nuclei and the cortex governs the rate of contraction, and that contraction can be induced by local solation. The shape of the cortex and the spatial relation of the nuclei within it therefore determine the pattern of cytoplasmic and nuclear movement. The mechanism we propose will deform the solated region surrounding the nuclei until that region is concentric with the cortical shell that anchors the actin network.

Does Such a Process Exist in Other Cells?

Counce (1973) refers to several examples of birectional cytoplasmic streaming in insect eggs, and fountain streaming and axial expansion take place in embryos of *Tribolium* (J. Hodin, personal communication). These phenomena and the proposed mechanisms for axial expansion (this paper) and cortical migration (Baker et al., 1993) may be general among the insects. The actin cytoskeleton of many embryos, including *C. elegans* (Strome, 1986) and *Boltenia*, an ascid-

ian (unpublished observations), resembles what we have described in *Drosophila*: a dense granular cortical layer and a less dense fibrous network extending into the cytoplasm. Cytoplasmic streaming has also been documented in these and other embryos (Hird and White, 1993; Rappaport and Rappaport, 1988; our unpublished observations). Taylor and colleagues have demonstrated the application of solation-contraction coupling not only to amoeba but also to motility of cultured mammalian cells, and have shown that actin polymerizes into a network near the periphery of the interphase cell and disassembles in the vicinity of the nucleus (Kolega et al., 1991; Giuliano and Taylor, 1994). Furthermore, Taylor and Fechheimer (1982) pointed out that solation-induced contraction within the cortical cytoskeleton could be invoked to rephrase models for cytokinesis such as the polar relaxation model (White and Borisy, 1983). In principle, any cell possessing an actin/myosin network within its cytoplasm might rearrange its components at will or in response to a signal by locally modulating the relative degree of assembly of the contractile network.

We thank Jayne Baker, Rob Baker, Rachel Collin, Victoria Foe, Jason Hodin, Lisa Maves, Ed Munro, Mark Mooseker, Andrew Murray, Garry Odell, David Pritchard, Bill Theurkauf, and two anonymous reviewers for critically reviewing the manuscript. We wish especially to acknowledge the continuing contribution of Victoria Foe, Ed Munro, and Garry Odell to the development of the hypotheses we present. We thank Jayne Baker for assistance and advice throughout this work and for performing the embryo injections analyzed in this paper, and we thank Liza von Dassow for photography.

This work was supported by National Institutes of Health grant GM 33656 to G. Schubiger and by a National Science Foundation predoctoral fellowship to G. von Dassow.

Received for publication 25 July 1994 and in revised form 9 September 1994.

References

Allen, R. D. 1961. Ameboid movement. *In* The Cell. J. Brachet and A. E. Mirsky, editors, Academic Press Inc., Orlando, FL. 135–216.

Allen, R. D. 1973. Biophysical aspects of pseudopod formation and retraction. *In* The Biology of Amoeba. K. W. Jeon, editor. Academic Press Inc., Orlando, FL. 201–247.

Baker, J., W. E. Theurkauf, and G. Schubiger. 1993. Dynamic changes in microtubule configuration correlate with nuclear migration in the preblastoderm *Drosophila* embryo. *J. Cell Biol.* 122:113–121.

Counce, S. J. 1973. The casual analysis of insect embryogenesis. *In* Developmental Systems: Insects. S. J. Counce and C. H. Waddington, editors. Academic Press Inc., Orlando, FL. 1–156.

Edgar, B. A., and G. Schubiger. 1986. Parameters controlling transcriptional activation during early *Drosophila* development. *Cell.* 44:871–877.

Foe, V. E., and B. M. Alberts. 1983. Studies of nuclear and cytoplasmic behavior in the five mitotic cycles that precede gastrulation in *Drosophila* embryogenesis. *J. Cell Sci.* 61:31–70.

Foe, V. E., G. M. Odell, and B. A. Edgar. 1993. Mitosis and morphogenesis in the *Drosophila* embryo: point and counterpoint. *In* The Development of *Drosophila melanogaster*. M. Bate and A. Martinez-Arias, editors. Cold Spring Harbor Laboratory Press, Cold Spring Harbor, New York. 149–300.

Giuliano, K. A., and D. L. Taylor. 1994. Fluorescent actin analogs with a high affinity for profilin in vitro exhibit an enhanced gradient of assembly in living cells. *J. Cell Biol.* 124:971–983.

Hatanaka, K., and M. Okada. 1991. Retarded nuclear migration in *Drosophila* embryos with aberrant F-actin reorganization caused by maternal effect mutations and by cytochalasin treatment. *Development (Camb.).* 111:909–920.

Hird, S. N., and J. G. White. 1993. Cortical and cytoplasmic flow polarity in early embryonic cells of *C. elegans*. *J. Cell Biol.* 121:1343–1355.

Janson, L. W., and D. L. Taylor. 1993. In vitro models of tail contraction and cytoplasmic streaming in amoeboid cells. *J. Cell Biol.* 123:345–356.

Janson, L. W., J. Kolega, and D. L. Taylor. 1991. Modulation of contraction by gelation/solation in a reconstituted motile model. *J. Cell Biol.* 114: 1005–1015.

Kolega, J., L. W. Janson, and D. L. Taylor. 1991. The role of solation-contraction coupling in regulating stress fiber dynamics in nonmuscle cells. *J. Cell Biol.* 114:993–1003.

Odell, G.M. 1977. Amoeboid motions. *Lect. Appl. Math.* 16:191–220.

Oster, G. F., and G.M. Odell. 1984. The mechanochemistry of cytogels. *Physica.* 12D:333–350.

Rabinowitz, M. 1941. Studies on the cytology and early embryology of the egg in *Drosophila melanogaster*. *J. Morphol.* 69:1–49.

Rappaport, R., and B. N. Rappaport. 1988. Reversing cytoplasmic flow in nucleated, constricted sand dollar eggs. *J. Exp. Zool.* 247:92–98.

Schliwa, M. 1982. Action of cytochalasin D on cytoskeletal networks. *J. Cell Biol.* 92:79–91.

Schubiger, G., and B. A. Edgar. 1994. Using inhibitors to study embryogenesis. *In Drosophila melanogaster*. Practical Uses in Cell and Molecular Biology. Methods in Cell Biology Series. L. S. B. Goldstein and E. A. Fyrberg, editors. Academic Press, Inc., Orlando, FL.

Stossel, T. P. 1993. On the crawling of animal cells. *Science (Wash. DC).* 260:1086–1093.

Strome, S. 1986. Fluorescence visualization of the distribution of microfilaments in gonads and early embryos of the nematode *Caenorhabditis elegans*. *J. Cell Biol.* 103:2241–2252.

Taylor, D. L., and M. Fechheimer. 1982. Cytoplasmic structure and contractility: the solation-contraction hypothesis. *Phil. Trans. R. Soc. Lond. B. Biol. Sci.* 299:185–197.

Taylor, D. L., J. S. Condeelis, P. L. Moore, and R. D. Allen. 1973. The contractile basis of amoeboid movement. I. The chemical control of motility in isolated cytoplasm. *J. Cell Biol.* 59:378–394.

Toyama, S., and S. Toyama. 1988. Functional alterations in β' actin from a KB cell mutant resistant to cytochalasin B. *J. Cell Biol.* 107:1499–1504.

The United Nations Educational, Scientific, and Cultural Organization (UNESCO). 1958. 700 Science Experiments for Everyone. Doubleday and Company, Inc., Garden City, NY. 250 pp.

Weir, M. P., B. A. Edgar, T. A. Kornberg, and G. Schubiger. 1988. Spatial regulation of *engrailed* expression in the *Drosophila* embryo. *Genes & Dev.* 2:1194–1203.

White, J. G., and G. G. Borisy. 1983. On the mechanism of cytokinesis in animal cells. *J. Theor. Biol.* 101:289–316.

Yasuda, G. K., J. Baker, and G. Schubiger. 1991. Independent roles of centrosomes and DNA in organizing the *Drosophila* cytoskeleton. *Development (Camb.).* 111:379–391.

Young, P. E., T. C. Pesacreta, and D. P. Kiehart. 1991. Dynamic changes in the distribution of cytoplasmic myosin during *Drosophila* embryogenesis. *Development (Camb.).* 111:1–14.

Zalokar, M., and I. Erk. 1976. Division and migration of nuclei during early embryogenesis of *Drosophila melanogaster*. *J. Microsc. Biol. Cell.* 25: 97–106.